

**Abstract.** We report the results of search for a point X-ray source (stellar remnant) in the southwest protrusion of the supernova remnant G 315.4–2.30 (MSH 14–63, RCW 86) using the archival data of the *Chandra X-ray Observatory*. The search was motivated by a hypothesis that G 315.4–2.30 is the result of an off-centered cavity supernova explosion of a moving massive star, which ends its evolution just near the edge of the main-sequence wind-driven bubble. This hypothesis implies that the southwest protrusion in G 315.4–2.30 is the remains of a preexisting bow shock-like structure created by the interaction of the supernova progenitor’s wind with the interstellar medium and that the actual location of the supernova blast center is near the center of this hemispherical structure. We have discovered two point X-ray sources in the “proper” place. One of the sources has an optical counterpart with the photographic magnitude  $13.38 \pm 0.40$ , while the spectrum of the source can be fitted with an optically thin plasma model. We interpret this source as a foreground active star of late spectral type. The second source has no optical counterpart to a limiting magnitude  $\sim 21$ . The spectrum of this source can be fitted equally well with several simple models (power law: photon index  $\simeq 1.87$ ; two-temperature blackbody:  $kT_1 = 0.11$  keV,  $R_1 = 2.34$  km and  $kT_2 \simeq 0.71$  keV,  $R_2 = 0.06$  km; blackbody plus power law:  $kT = 0.07$  keV, photon index  $\simeq 2.3$ ). We interpret this source as a candidate stellar remnant (neutron star), while the photon index and nonthermal luminosity of the source (almost the same as those of the Vela pulsar and recently discovered pulsar PSR J0205+6449 in the supernova remnant 3C 58) suggest that it can be a young “ordinary” pulsar.

**Key words:** Stars: neutron – ISM: bubbles – ISM: individual objects: G 315.4–2.30 (MSH 14–63, RCW 86) – ISM: supernova remnants – X-ray: stars

# Point X-ray sources in the SNR G 315.4–2.30 (MSH 14–63, RCW 86)

V.V. Gvaramadze<sup>1,2,3\*</sup> and A.A. Vikhlinin<sup>4</sup>

<sup>1</sup> Sternberg Astronomical Institute, Moscow State University, Universitetskij Pr. 13, Moscow, 119992, Russia

<sup>2</sup> E.K.Kharadze Abastumani Astrophysical Observatory, Georgian Academy of Sciences, A.Kazbegi ave. 2-a, Tbilisi, 380060, Georgia

<sup>3</sup> Abdus Salam International Centre for Theoretical Physics, Strada Costiera 11, P.O. Box 586, 34100 Trieste, Italy

<sup>4</sup> Space Research Institute, Russian Academy of Sciences, Profsoyuznaya 84/32, Moscow, 117997, Russia

Received / accepted

## 1. Introduction

G 315.4–2.30 (MSH 14–63, RCW 86) is a bright (in both radio and X-rays) shell-like supernova remnant (SNR) with a peculiar protrusion in the southwest (e.g. Dickel et al. 2001, Vink et al. 1997). This protrusion coincides with a bright hemispherical optical nebula (Rodger et al. 1960, Smith 1997; see also Fig. 3). The characteristic angular size of the SNR is about 40', that at a distance to the remnant of 2.8 kpc (Rosado et al. 1996) corresponds to  $\simeq 32$  pc. The radius of the optical nebula is  $\simeq 2'$  (or  $\simeq 1.6$  pc). A collection of observational data points to the youth (few thousand years) of the SNR (see e.g. Dickel et al. 2001).

Vink et al. (1997) put forward an idea that the SNR G 315.4–2.30 is the result of a supernova (SN) explosion inside a preexisting wind-driven cavity (see also Dickel et al. 2001, Vink et al. 2002) and noted that the elongated shape of the SNR reminds that of a wind-driven cavity created by a *moving* massive star (see Weaver et al. 1977 and Brighenti & D'Ercole 1994 for details). On the other hand, it is believed that the origin of the southwest protrusion is due to the interaction of the SN blast wave with a density enhancement in the ambient interstellar medium. However, as were correctly noted by Dickel et al. (2001), the density enhancement (e.g. a high-density cloud) should result in a concave dent in the shell, not in the protrusion. Dickel et al. (2001) also suggested that this protrusion “is perhaps the key to what is going on”.

We agree with the idea that G 315.4–2.30 is a diffuse remnant of an off-centered cavity SN explosion and supplement it by a suggestion that the massive SN progenitor star explodes just near the edge of the main-sequence bubble. This suggestion implies that the southwest protrusion is the remains of a bow shock-like structure created in the

interstellar medium by the post-main-sequence winds (see Sect. 4 and Gvaramadze 2002; cf. Wang et al. 1993) and that the SN exploded near the center of this hemispherical structure. Given the youth of the SNR and assuming a reasonable kick velocity for the stellar remnant, one can expect that the stellar remnant should be still within the protrusion. Motivated by these arguments Gvaramadze (2002) searched for a possible compact X-ray source in the southwest of G 315.4–2.30 using the *ROSAT* archival data, but the moderate spatial resolution of the *ROSAT* PSPC precluded detection of point sources against the bright background emission of the SNR's shell.

In this paper we report the discovery of two point X-ray sources near the center of the hemispherical optical nebula using the archival Advanced CCD Imaging Spectrometer (ACIS) data of the *Chandra X-Ray Observatory*. We interpret one of the sources as a foreground active star of late spectral type, while the second one as a candidate stellar remnant (neutron star).

## 2. Point X-ray sources

### 2.1. X-ray images

Fig. 1 shows the *Chandra* (0.7–2 keV) image of the highly structured southwest corner of the SNR G 315.4–2.30. Two point X-ray sources are clearly visible at the northwest of the image at  $\alpha_{2000} = 14^{\text{h}}40^{\text{m}}31^{\text{s}}.33$ ,  $\delta_{2000} = -62^{\circ}38'22''$  and  $\alpha_{2000} = 14^{\text{h}}40^{\text{m}}31^{\text{s}}.05$ ,  $\delta_{2000} = -62^{\circ}38'16''$ . Fig. 2 shows a close-up of the region around the sources, labelled as S (southern source) and N (northern source).

### 2.2. Optical images

Fig. 3 shows the image of the hemispherical optical nebula in the southwest of the SNR G 315.4–2.30 from the Digital Sky Survey (DSS-2, red plates). Fig. 4 shows an enlarged view of the region around the point X-ray sources. The

Send offprint requests to: V.V. Gvaramadze

\* Address for correspondence: Krasin str. 19, ap. 81, Moscow, 123056, Russia (vgvaram@sci.msu.ru)

**Fig. 1.** *Chandra* image of the southwest region of the SNR G 315.4–2.30. Both X-ray sources are surrounded by a circle. North is up and east is to the left.

**Fig. 2.** The enlarged view of the region around the point X-ray sources, labelled as S (southern) and N (northern).

**Fig. 3.** The DSS-2 image of the optical nebula in the southwest of the SNR G 315.4–2.30. The position of both point X-ray sources is surrounded by a circle.

source S is in a good positional agreement with a point-like object immersed in a diffuse optical filament. This object is indicated in the HST Guide Star Catalog as a non-stellar one, with the photographic magnitude  $13.38 \pm 0.40$ . We believe, however, that it was misclassified due to the effect of the background diffuse emission and in fact it is a star. The source N has no optical counterpart to a limiting magnitude  $\sim 21$ .

### 2.3. Spectral analysis

For the spectral analysis we have used the archival ACIS data. The spectra of the point sources were extracted from circular regions with radii of 1.5 arcsec. The background spectrum was taken from a circle with a radius of 4.5 arcsec at 5 arcsec northeast from the point sources. The spectral modeling was performed in the 0.5–10 keV energy range using the XSPEC spectra fitting package. The estimates of the interstellar absorption,  $N_{\text{H}}$ , towards G 315.4–2.30 are quite uncertain (cf. e.g. Vink et al. 1997 with Vink et al. 2002), so the spectra were fitted with  $N_{\text{H}}$  as a free parameter. In one case, however, we used the fixed value of  $N_{\text{H}}$  (see below).

The spectrum of the source S is shown in Fig. 5; the solid line represents the best fit optically thin plasma model, with the temperature  $= 0.69 \pm 0.05$  keV, abundance  $= 0.07 \pm 0.02$ ,  $N_{\text{H}} = (1.2 \pm 0.3) \times 10^{21} \text{ cm}^{-2}$ , and luminosity (in the 0.5–10 keV energy range)  $\simeq 2.8 \times 10^{31} \text{ erg s}^{-1}$ . The blackbody or power law models give unacceptable fits.

The spectrum of the source N (shown in Fig. 6) can be fitted equally well with a power law (PL), two-temperature blackbody (BB+BB), or blackbody plus power law (BB+PL) models. A simple BB model gives unacceptable fits. The best fit spectrum predicted by the BB+PL model is shown in Fig. 6 by the solid line.

We note that the best fit PL model requires  $N_{\text{H}} = 0$  (we consider this fact as an indication of the galactic origin of the source N), although models with  $N_{\text{H}}$  up to  $1.5 \times 10^{21} \text{ cm}^{-2}$  (presented in Table 1) also give acceptable fits.

The results of spectral analysis for the source N are summarized in Table 1.

## 3. Discussion

### 3.1. Source S

The soft X-ray spectrum of the source S and the existence of the optical counterpart strongly suggest that this source is an active star. Assuming that S is indeed a star and given the observed X-ray to optical flux ratio, one can exclude a possibility that this star is of OB-type. Therefore it cannot be a member of a group of OB stars located in the direction of G 315.4–2.30 nearly at the same distance as the SNR (Westerlund 1969). Most likely the source S is a foreground active star of late spectral type. The follow-up study of this object can clarify its nature.

### 3.2. Source N

The spectral characteristics of the source N coupled with the absence of an optical counterpart allow to consider it as a candidate stellar remnant.

The PL fit of the spectrum (with the photon index typical of pulsars) suggest that the source N can be an active (rotation-powered) neutron star. Assuming that N is a pulsar<sup>1</sup> and using the empirical relationships between the nonthermal X-ray and spin-down luminosities of pulsars (e.g. Becker & Trümper 1997, Possenti et al. 2002), one can estimate the latter,  $\dot{E} \sim 10^{35} d_{2.8}^2 \text{ erg s}^{-1}$ , where  $d_{2.8}$  is the distance to the SNR in units of 2.8 kpc.

The inferred low spin-down luminosity can be considered as an argument against a possibility that the source N is a young fast-rotating pulsar with a standard magnetic field ( $10^{11} - 10^{13}$  G)<sup>2</sup>. Therefore N can be either a young pulsar born with a low surface magnetic field (e.g. Blandford et al. 1983, Urpin et al. 1986) and/or large rotation period (e.g. Spruit & Phinney 1998) or an aged pulsar with decaying magnetic field. The first possibility would deserve a detailed consideration if a candidate period of 12 ms found for the central X-ray source in Cas A

<sup>1</sup> The 3.2 s individual exposure time of the ACIS instrument makes impossible the search for short pulsations.

<sup>2</sup> Note, however, that the 267 ms radio pulsar PSR B 1853+01 associated with the mixed-morphology SNR W 44 (Wolszczan et al. 1991) has almost the same spin-down luminosity ( $\simeq 4 \times 10^{35} \text{ erg s}^{-1}$ ), while the characteristic age of the pulsar ( $\simeq 2 \times 10^4$  yr) points to its youth. On the other hand, this pulsar could be much older if its high spin-down rate ( $\dot{P} \simeq 0.2 \times 10^{-12} \text{ ss}^{-1}$ ) is connected with the interaction between the pulsar's magnetosphere and the dense circumstellar matter (cf. Gvaramadze 2001).

**Fig. 4.** The enlarged DSS-2 image of the region around the point X-ray sources. The circles are centered at the positions of X-ray sources.

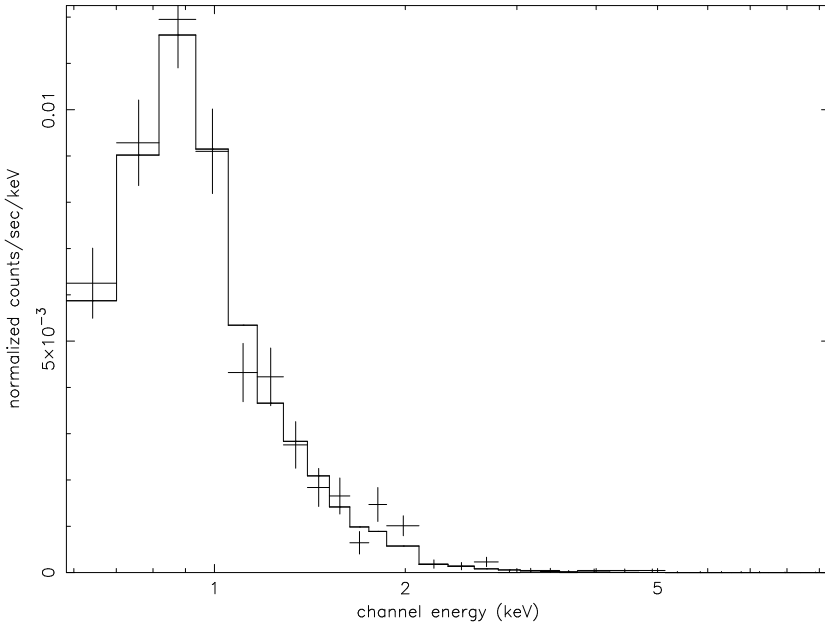


**Fig. 5.** The background-subtracted *Chandra* ACIS spectrum from the source S. The solid line represents the best fit optically thin plasma model.

**Table 1.** Spectral fits to the point X-ray source N.

Model	Photon index	Temperature, keV	$N_{\text{H}}$ , $10^{21} \text{ cm}^{-2}$	Luminosity, $10^{32} \text{ erg s}^{-1}$
PL	$1.87 \pm 0.09$		1.5 (fixed)	0.44 (0.5 – 10 keV)
B+B		$0.11 \pm 0.03$	$4.3 \pm 1.8$	1.32 (bolometric)
		$0.71 \pm 0.05$		0.35 (bolometric)
BB+PL		$0.070 \pm 0.003$	$9.2 \pm 3.4$	112 (bolometric)
	$2.31 \pm 0.30$			0.67 (0.5 – 10 keV)

(Murray et al. 2002a) will be confirmed by an independent timing analysis. The second one implies that N is an old pulsar (of an arbitrary age) projected by chance on the SNR G 315.4–2.30, or that is more plausible it was a binary with the SN progenitor star. In the latter case, the old pulsar is a by-product of the second SN explosion in a massive binary system and the age of the pulsar

should not much exceed  $\sim 10^6$  yr, i.e. the time elapsed after the first SN explosion. For this age and the spin-down luminosity estimated above, one has the pulsar rotation period,  $P = (2\pi^2 I/\tau \dot{E})^{1/2} \simeq 8$  ms and surface magnetic field,  $B = (3c^3 I P^2 / 16\pi\tau R^6)^{1/2} \simeq 6 \times 10^{11}$  G (here we assumed that the pulsar age is equal to the characteristic one,  $\tau = P/2\dot{P}$ ;  $I = 10^{45} \text{ g cm}^2$  and  $R = 10^6 \text{ cm}$  are,

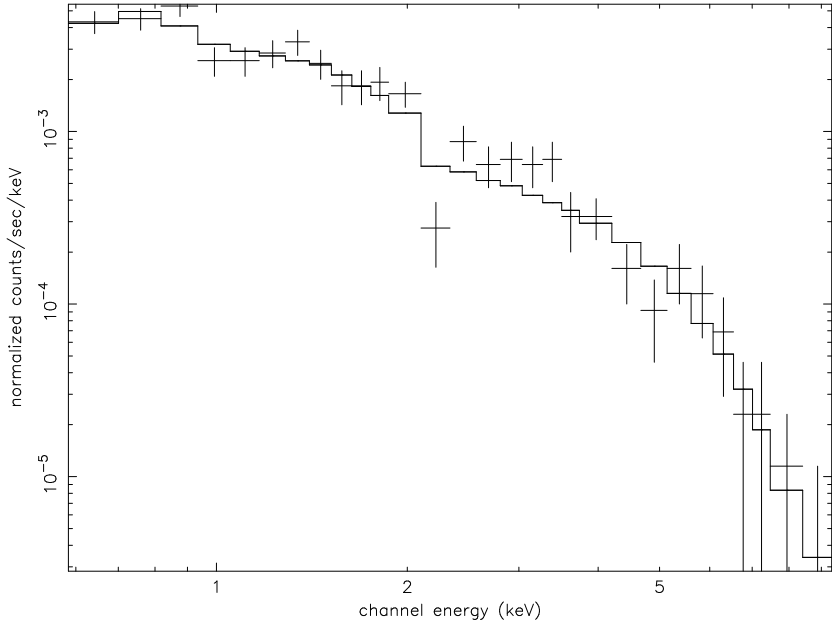


**Fig. 6.** The background-subtracted *Chandra* ACIS spectrum from the source N. The solid line corresponds to the best fit blackbody plus power law model.

respectively, the moment of inertia and radius of the pulsar). In this scenario, a second (young) stellar remnant (not necessary an active pulsar) should exist nearby.

Note, however, that the above-mentioned empirical relationships are quite uncertain and should be used with caution. For example, the spin-down luminosity of the recently discovered young (characteristic age  $\simeq 5400$  yr) pulsar PSR J 0205+6449 in the SNR 3C 58 is  $2.6 \times 10^{37}$  erg s $^{-1}$  (Murray et al. 2002b), while its (nonthermal; see Slane et al. 2002) X-ray luminosity is  $\simeq 2.1 \times 10^{32} d_{2.6}^2$  erg s $^{-1}$ , i.e. about two orders of magnitude less than that predicted by the empirical relationships. The disparity between the predicted and observed nonthermal luminosities is even higher in the case of the Vela pulsar (Pavlov et al. 2001). Note also that the photon indecies and nothermal luminosities of these two pulsars are almost the same as those predicted for the source N by the PL (or BB+PL) model, while their characteristic ages are of the same order of magnitude as the age of the SNR G 315.4–2.30 inferred in Sect. 4. Therefore one cannot exclude that the source N is a young pulsar with “ordinary” parameters. This should be tested observationally.

In the two-temperature blackbody model, the origin of the soft component can be attributed to the cooling surface of a neutron star, while the hard component – to the polar caps heated by the backflow of relativistic particles (e.g. Wang et al. 1998). The best fit BB+BB model yields the temperature of the soft component of  $\simeq 0.11$  keV and the effective radius of 2.3 km. The inferred temperature is somewhat larger than that predicted by standard cooling models (e.g. Page 1998), while the radius is significantly smaller than the radius of the neutron star. In principle, one can expect that the use of realistic neutron star atmosphere models (e.g. Pavlov et al. 1995) would adjust these parameters to acceptable values. But the interpretation of the hard component is more problematic. The effective polar cap area inferred from the best fit BB+BB model ( $\sim 10^8$  cm $^{-2}$ ) is too small and observed temperature is too large to be consistent with models for heating of polar caps (e.g. Wang et al. 1998 and references therein). Therefore we consider this model as unphysical and suggest that at least at high energies the X-ray emission of the source N is nonthermal.

The use of the BB+PL model assumes that the soft X-ray emission comes from the entire surface of a cool-

ing neutron star or from some smaller hot areas, while the hard X-rays are due to the nonthermal magnetospheric emission. The best fit BB+PL model shows that the spectrum of the source N is dominated by the non-thermal emission at energies  $> 1$  keV and suggests the existence of a soft thermal component. However, the unknown interstellar absorption and uncertainties due to the time-dependent decrease in ACIS low-energy quantum efficiency make the estimates of the flux and bolometric luminosity of the BB component unconstrained. The best fit model with  $N_{\text{H}}$  as a free parameter (see Table 1) requires large interstellar absorption<sup>3</sup> and a consequent large bolometric luminosity. Although the large absorption is consistent with values derived by Vink et al. (2002) for the SNR G 315.4–2.30, the large inferred bolometric luminosity implies an uncomfortably large effective radius of  $\simeq 60$  km. The normalization of the BB component, however, is plausible for lower values of  $N_{\text{H}}$ . A more detailed consideration of this problem will be possible only with updated *Chandra* calibration at low energies.

In conclusion we note that at present we cannot firmly confirm or reject the existence of a soft BB component, and therefore we consider the PL model with a reasonable  $N_{\text{H}}$  as a good approximation for the spectrum of the source N. The follow-up multiwavelength observations of this source, including the search for pulsed emission, long-term variability, and radio, optical or  $\gamma$ -ray counterparts may provide a crucial information for the understanding of its nature and therefore are highly desirable.

#### 4. SNR G 315.4–2.30

We now briefly discuss a scenario for the origin of the SNR G 315.4–2.30 (the more detailed description will be presented elsewhere). We note that our scenario have many in common with the model proposed by Wang et al. (1993) to explain the origin of large-scale structures around the SN 1987A, and suggest that G 315.4–2.30 is an older version of the former.

We believe that the SNR G 315.4–2.30 is the result of a cavity SN explosion of a moving massive star and that after the main-sequence (MS) phase (lasting  $\sim 10^7$  yr) the SN progenitor have evolved through the red supergiant (RSG) phase ( $\sim 10^6$  yr) and then experienced a short ( $\sim 10^4$  yr) “blue loop”, i.e. the zero-age MS mass of the star was  $15 - 20 M_{\odot}$ . During the MS phase the stellar wind (with the mechanical luminosity,  $L$ , of  $\sim 10^{35}$  erg s $^{-1}$ )

<sup>3</sup> Note that dense clumps of circumstellar matter (the natural products of interaction between post-main-sequence winds of the SN progenitor star [Gvaramadze 2001 and references therein]; see also Sect. 4) could add a significant contribution to the neutral hydrogen absorption towards the source N, as well as the enhanced absorption towards the central compact source in Cas A (required by some model fits of its spectrum; e.g. Murray et al. 2002a) might be caused by the dense circumstellar gas of a foreground floccule (cf. Gvaramadze 2001).

blows up in the interstellar medium a large-scale bubble which eventually (at time  $t_{\text{st}} \simeq 10^6 (L_{35}/n)^{1/2}$  yr, where  $L_{35} = L/10^{35}$  erg s $^{-1}$  and  $n$  is the number density of the interstellar gas) stalls at radius  $R_{\text{st}} \simeq 14 (L_{35}/n)^{1/2}$  pc (we recall that the radius of the SNR G 315.4–2.30 is  $\simeq 16$  pc). The stellar motion results in that the star crosses the stalled bubble and starts to interact directly with the unperturbed interstellar gas. This happens at time  $t_{\text{cr}} \simeq R_{\text{st}}/v_{\star} = 2.7 \times 10^6 (L_{35}/n)^{1/2} v_{\star,5}^{-1}$  yr, where  $v_{\star,5}$  is the stellar velocity in units of 5 km s $^{-1}$ , which is comparable with the duration of the MS phase if  $v_{\star} \simeq 1 - 2$  km s $^{-1}$ . In this case the SN progenitor star enters in the RSG phase while it was just near the edge of the MS bubble. During the relatively short RSG phase the star losses most (two thirds) of its initial mass in the form of dense, slow wind. The interaction of the RSG wind with the interstellar medium results in the origin of a bow shock-like structure with a characteristic radius,  $r$ , determined by the relationship:  $\dot{M}_{\text{RSG}} v_{\text{RSG}} / 4\pi r^2 = n(2kT + m_{\text{H}}v_{\star}^2)$ , where  $\dot{M}_{\text{RSG}}$  and  $v_{\text{RSG}}$  are, correspondingly, the mass-loss rate and wind velocity during the RSG stage,  $T$  is the temperature of the ambient interstellar medium,  $k$  is the Boltzmann constant, and  $m_{\text{H}}$  is the mass of a hydrogen atom. For  $n \simeq 1$  cm $^{-3}$  (Smith 1997, Ghavamian et al. 2001),  $\dot{M}_{\text{RSG}} = 10^{-5} M_{\odot}$  yr $^{-1}$ ,  $v_{\text{RSG}} = 10$  km s $^{-1}$ ,  $T = 8000$  K, and  $v_{\star} = 2$  km s $^{-1}$ , one has  $r \simeq 1.5$  pc. This value is in a comfortable agreement with the radius of the hemispherical optical nebula in the southwest of G 315.4–2.30 ( $\simeq 1.6$  pc).

About  $\sim 10^4$  yr before the SN explosion the progenitor star becomes a blue supergiant, whose fast wind sweeps the material of the RSG wind. We speculate that at the moment of SN explosion the blue supergiant wind was trapped in the southwest direction by the dense material of the bow shock-like structure, while in the opposite direction it was able to break out in the low-density MS bubble, so that the SN explodes inside a hollow hemispherical structure opened towards the MS bubble.

The SN blast wave passes almost freely across the low-density MS bubble (for the explosion energy of  $E = 10^{51}$  erg and mass of the SN ejecta of  $\simeq 3.5 M_{\odot}$ , the expansion velocity of the blast wave is  $\simeq 5000$  km s $^{-1}$ ) and reaches the current position in the northeast after  $\sim 6 \times 10^3$  yr. The density jump at the edge of the bubble results in the abrupt deceleration of the blast wave to a velocity of  $\simeq 600 - 800$  km s $^{-1}$  (these values were derived from studies of Balmer-dominated filaments encircling the SNR G 315.4–2.30; Long & Blair 1990, Smith 1997). This deceleration implies the density jump by a factor of  $\simeq 40 - 70$  or the number density of the MS bubble gas  $n_{\text{b}} \simeq 0.01 - 0.03$  cm $^{-3}$ , i.e. a reasonable value given the number density of the ambient interstellar gas of  $\simeq 1$  cm $^{-3}$  (see e.g. Weaver et al. 1977).

In the southwest direction, however, the expansion of the SN blast wave is hampered by the dense hemispherical circumstellar shell. The shocked remains of this shell

are now seen as the bright southwest protrusion (shown in Fig. 3). The existence of radiative filaments in this corner of the SNR implies that the blast wave slows down to the velocity of  $\simeq 100 \text{ km s}^{-1}$ , that in its turn implies the density contrast of 2500. For  $n_b = 0.02 \text{ cm}^{-3}$ , one has the number density of the circumstellar material of  $\sim 50 \text{ cm}^{-3}$ , i.e. in a good agreement with the density estimate derived by Leibowitz & Danziger (1983). On the other hand, the recent discovery of Balmer-dominated filaments protruding beyond the radiative arc (see Fig. 3 of Smith 1997), suggests that the SN blast wave partially overrun the clumpy circumstellar shell (cf. Franco et al. 1991) and now propagates through the interstellar medium. For the radial extent of protrusions of  $\simeq 2 \text{ pc}$  and assuming that the mean expansion velocity is  $\sim 700 \text{ km s}^{-1}$ , one has that the blowouts are occurred  $\sim 3 \times 10^3 \text{ yr}$  ago.

## 5. Conclusion

We have analyzed the archival *Chandra X-Ray Observatory* data on G 315.4–2.30 to search for a stellar remnant in the southwest corner of this SNR. The search was motivated by a hypothesis that the SNR G 315.4–2.30 is the result of an off-centered cavity SN explosion of a moving massive star, which ends its evolution just near the edge of the main-sequence wind-driven bubble. This hypothesis implies that the southwest protrusion in G 315.4–2.30 is the shocked material of a preexisting circumstellar structure and that the actual location of the SN blast center is near the center of this structure. We have discovered two point X-ray sources in the “proper” place. One of the sources is interpreted as a foreground active star of late spectral type, while the second one as a candidate neutron star (perhaps a young “ordinary” pulsar). The follow-up observations of these sources will help to understand their nature and thereby to test the hypothesis on the origin of the SNR G 315.4–2.30.

## References

Becker, W., & Trümper, J., 1997, A&A, 326, 682

Blandford, R.D., Applegate J.H., & Hernquist L., 1983, MNRAS, 204, 1025

Brightenti, F., & D’Ercole, A., 1994, MNRAS, 270, 65

Dickel, J.R., Strom, R.G., & Milne, D.K., 2001, ApJ, 546, 447

Franco, J., Tenorio-Tagle, G., Bodenheimer, P., & Rózyczka, M., 1991, PASP, 103, 803

Ghavamian, P., Raymond, J., Smith, C.R., & Hartigan, P., 2001, ApJ, 547, 995

Gvaramadze, V.V., 2001, A&A, 374, 259

Gvaramadze, V.V., 2002, in New Visions of the X-ray Universe in the XMM-Newton and Chandra Era, ed. F. Jansen, ESA SP-488, in press (astro-ph/0208028)

Leibowitz, E.M., & Danziger, I.J., 1983, MNRAS, 204, 273

Long, K.S., & Blair, W.P., 1990, ApJ, 358, L13

Murray, S.S., Ransom, S.M., Juda, M., Hwang, U., & Holt, S.S., 2002a, ApJ, 566, 1039

Murray, S.S., Slane, P.O., Seward, F.D., Ranson S.M., & Gaensler, B.M., 2002b, ApJ, 568, 226

Page, D., 1998, in The Many Faces of Neutron Stars, eds. R. Buccieri, J. van Paradijs, & M.A. Alpar (Kluwer:Dordrecht), p. 539

Pavlov, G.G., Shibanov, Yu.A., Zavlin, V.E., & Meyer, R.D., 1995, in The Lives of the Neutron Stars, eds. M.A. Alpar, Ü. Kiziloglu & J. van Paradijs (Kluwer:Dordrecht), p. 71

Pavlov, G.G., Zavlin, V.E., Sanwal, D., Burwitz, V., & Garmire, G.P., 2001, ApJ, 552, L129

Possenti, A., Cerutti, R., Colpi, M., & Mereghetti, S., 2002, A&A, 387, 993

Rodgers, A.W., Campbell, C.T., & Whiteoak, J.B., 1960, MNRAS, 121, 103

Rosado, M., Ambrocio-Cruz, P., Le Coarer, E., & Marcellin, M., 1996, A&A, 315, 243

Slane, P., Helfand, D.J., & Murray, S.S., 2002, ApJ, 571, L45

Smith, R.C, 1997, AJ, 114, 2664

Spruit, H., & Phinney, E.S., 1998, Nat, 393, 139

Urpin, V.A., Levshakov, S.A., & Yakovlev, D.G., 1986, MNRAS, 219, 703

Vink, J., Kaastra, J.S., & Bleeker, J.A.M., 1997, A&A, 328, 628

Vink, J., Bleeker, J., Kaastra, J., van der Heyden, K., & Dickel, J., 2002, in New Visions of the X-ray Universe in the XMM-Newton and Chandra Era, ed. F. Jansen, ESA SP-488, in press (astro-ph/0112216)

Wang, L., Dyson, J.E., & Kahn, F.D., 1993, MNRAS, 261, 391

Wang, F.Y.-H., Ruderman, M., Halpern, J.P., & Zhu, T., 1998, ApJ, 498, 373

Weaver, R., McCray, R., Castor, J., & Shapiro, P., 1977, ApJ, 218, 377

Westerlund, B.E., 1966, AJ, 74, 879

Wolszczan, A., Cordes, J.M., & Dewey, R.J., 1991, ApJ, 372, L99

This figure "fig1.jpg" is available in "jpg" format from:

<http://arxiv.org/ps/astro-ph/0208030v1>

This figure "fig2.jpg" is available in "jpg" format from:

<http://arxiv.org/ps/astro-ph/0208030v1>

This figure "fig3.jpg" is available in "jpg" format from:

<http://arxiv.org/ps/astro-ph/0208030v1>

This figure "fig4.jpg" is available in "jpg" format from:

<http://arxiv.org/ps/astro-ph/0208030v1>